We are IntechOpen, the world's leading publisher of Open Access books Built by scientists, for scientists

4,800
Open access books available

122,000
International authors and editors

135M
Downloads

Our authors are among the

154
Countries delivered to

TOP 1%
most cited scientists

12.2%
Contributors from top 500 universities

CLARIVATE ANALYTICS BOOK CITATION INDEX INDEXED

WEB OF SCIENCE™

Selection of our books indexed in the Book Citation Index in Web of Science™ Core Collection (BKCI)

Interested in publishing with us?
Contact book.department@intechopen.com

Numbers displayed above are based on latest data collected.
For more information visit www.intechopen.com

13

Removal Mechanisms in a Tropical Boundary Layer: Quantification of Air Pollutant Removal Rates Around a Heavily Afforested Power Plant

J. R. Picardo[1] and S. Ghosh[12]
[1]*School of Mechanical and Building Sciences, VIT University,*
[2]*ICAS Associate, School of Earth and Environment, University of Leeds*
[1]*India*
[2]*U.K.*

1. Introduction

Nature's astonishing biological resilience is closely linked to its self cleansing mechanisms. In a hugely populated developing world, economic growth comes with a heavy price. A multitude of industrial and transportation processes produce noxious gases which are released into the atmosphere. Fortunately many of these developing countries, like India, are blessed with a highly convective tropical boundary layer which dilutes pollution. In addition most of these developing Asian countries also receive intense monsoonal precipitations. Another common feature of these Asian nations is that their vegetative cover is dominated by evergreen plants, in contrast to many mid-latitude nations in the developed world where the number of evergreens are far limited. However, it is ironical that despite these natural propensities air pollution levels over Asian cities are much higher than their mid latitude counter parts. The purpose of this chapter is to describe, formulate and quantify the removal pathways of SO_2, a major air pollutant, through both dry and wet deposition whilst accounting for the endowments of nature enjoyed by tropical Asia. This is done via a detailed study on Asia's Largest Lignite based Power Plant- Neyveli Lignite Corporation (NLC) located in the Cuddalore district of Tamil Nadu in South India (Fig. 1). SO_2 is produced during the generation of power from lignite coal and released from elevated stacks (Table 1). An in depth modelling analysis of these emissions is presented addressing the dispersion of SO_2 in a tropical boundary layer using an atmospheric dispersion model developed as part of a consultancy with NLC and VIT University. The dry and wet deposition of the spatially distributed pollutant is then analyzed via suitable well established parameterizations. The quantification of removal mechanisms has a dual significance with respect to environmental studies. It is essential for calculating the atmospheric budget of trace gases as well as assessing the impact of emissions on local vegetation and structures due to acid deposition.

Two factors make NLC a particularly well suited study area for the purposes of this chapter; an extensive evergreen urban canopy and the North East (NE) monsoon which brings intense showers to the region from October to December. Regional climatology including year round high solar radiation and mild, almost non-existent, winters (temperature around

25 ^{0}C) make this a unique study. It is further set apart from investigations conducted in the mid-latitudes by the tropical vegetation and the intense monsoon showers which bear rain drops of larger mean diameter. All these factors are accounted for in the modelling analysis which is to follow, providing a basis for region specific environmental assessments. It will also serve as a roadmap for future studies in other Asian regions which have hitherto largely resorted to borrowing results from the mid-latitudes.

Fig. 1. Google Map showing the location of Neyveli Lignite Corporation (red A marker) in Tamil Nadu, India

Stack	Height (m)	SO_2 source strength (g s^{-1})
Thermal Power station-I		
1	60	227.82
2	60	271.35
3	60	153.23
4	120	305.99
Thermal Power station-I Expansion		
1	220	305.07
2	220	305.07
Thermal Power station-II		
1	170	359.38
2	170	359.38
3	170	359.38
4	220	317.45
5	220	317.45
6	220	317.45
7	220	317.45

Table 1. Details of stacks emitting SO_2 at NLC

2. Dry deposition

Deposition involves the transport of gaseous and particulate species from the atmosphere to physical surfaces at the ground where they are retained and thus removed from the atmosphere. In the absence of precipitation, they are brought to the surface by turbulent transport where they may be absorbed, adsorbed or chemically transformed. This process is called dry deposition. The deposition surface has a critical role to play and natural surfaces like vegetation, while difficult to describe in a study, promote dry deposition. This chapter is concerned with the mathematical modelling of SO_2 deposition. This section is devoted to the dry deposition of SO_2 onto a vegetative canopy while rain mediated removal is dealt with in the next section.

2.1 The urban canopy and the township at NLC

The founding fathers of NLC began a massive afforestation program which has resulted in the presence of 17 million tropical trees. The role of these trees in mitigating air pollution seems intuitive and a detailed quantitative investigation requires the application of dry deposition modelling techniques. Fig. 2 shows a map of NLC and an aerial view from Google Earth®. The region demarcated by a rectangle is the township of NLC which is home to 128,133 employees. Its proximity to the Thermal Power Station One (TPS1) makes it a particularly sensitive area which is likely to receive emissions from the stacks. Fortunately there is a considerable green cover over the township (Fig. 2) which promotes the deposition of pollutants and results in a cleaner atmosphere. The extent of this cleansing depends on the level of pollutant concentration and the environmental factors which modulate dry deposition. The quantification of the rate of dry deposition assumes greater significance in context of the health of the township's residents. The following sections are devoted towards this objective.

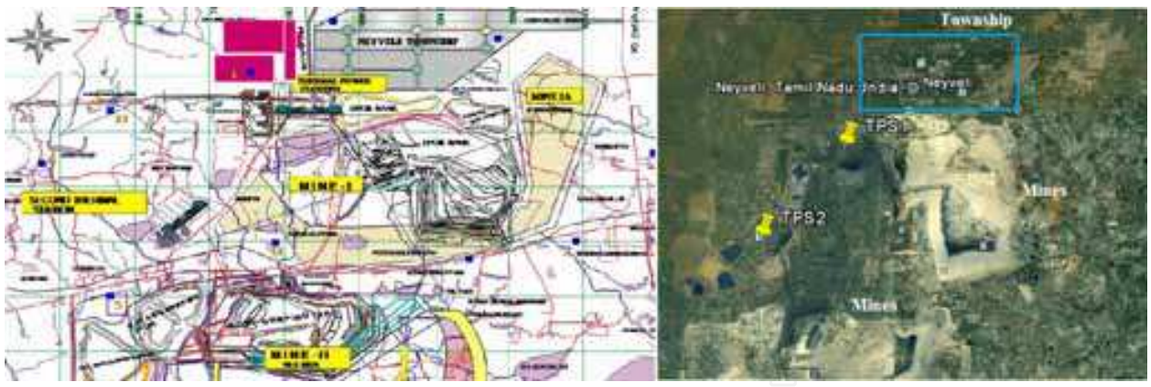

Fig. 2. Map of NLC and aerial view from Google Earth® of TPS1 and TPS2 and the Township (demarcated by a rectangle)

2.2 Parameterization of dry deposition to vegetation

The vegetative canopy is considered to be an irreversible sink for SO_2 and the flux of gas (F) to the ground is represented by a first order relationship. This flux is assumed to be uniform within the surface layer of the atmosphere (10-100 m) (Seinfeld and Pandis, 2006)

$$F = -V_d \times C_g \tag{1}$$

F has units of μg $m^{-2}s^{-1}$. C_g is the concentration of the gaseous species measured at a reference height within the surface layer (μg m^{-3}). V_d is a parameter called the deposition velocity and it has the units of m s^{-1} (hence the term velocity). Thus the problem of determining the flux of a species is transformed into the determination of its deposition velocity. The downward flux of the species is negative by convention and hence the deposition velocity is positive. Its value will depend on the reference height chosen and the assumption of uniform flux dictates that the concentration would also vary with height so as to keep the flux constant. The reference height in this study is taken to be 10 meters which is close to the vegetative surfaces (ensuring better agreement with the constant flux assumption) and is the height at which instrumentation is installed by NLC for meteorological and concentration measurements.

2.2.1 Deposition velocity- theory of resistances

The process of dry deposition is usually divided into three stages:

1. Transportation from the free atmosphere to the receptor surface (turbulent layer transport)
2. Transport through the quasi-laminar, stagnant air layer near the receptor surface (diffusive molecular transport)
3. Capture or absorption by the surface (in this case transport into the leaf stomata or cuticle or deposition onto the ground).

According to the universally adopted inferential resistance modelling approach, the dry deposition process is treated analogously to the flow of electrical current through a network of resistances in series. In this analogy, the aerodynamic resistance (R_a), the quasi-laminar resistance (R_b) and the surface resistance (R_c) refer to the aforementioned three stages of dry deposition respectively (all have units of s m^{-1}). The inverse of the total resistance is the dry deposition velocity (V_d).

$$V_d = \left(R_a + R_b + R_c\right)^{-1} \tag{2}$$

The aerodynamic component of the overall dry deposition resistance is typically based on gradient-transport theory and mass-transfer/momentum-transfer similarity. The resistance varies with the state of stability of the atmosphere. The quasi-laminar resistance depends on the diffusivity of the gas as well as the wind conditions. The aerodynamic and quasi-laminar resistances are computed by the following expressions (Seinfeld and Pandis, 2006). These expressions are valid only in the surface layer of the atmosphere where the species flux is constant. An approximate vertical extent is 100 m.

$$R_a = \begin{cases} \dfrac{1}{\kappa u_*}\left[\ln\left(\dfrac{z}{z_o}\right) + 4.7\left(\zeta - \zeta_0\right)\right] & (stable) \\ \dfrac{1}{\kappa u_*}\ln\left(\dfrac{z}{z_o}\right) & (neutral) \\ \dfrac{1}{\kappa u_*}\left[\ln\left(\dfrac{z}{z_o}\right) + \ln\left(\dfrac{\left(\eta_0{}^2+1\right)\left(\eta_0+1\right)^2}{\left(\eta_r{}^2+1\right)\left(\eta_r+1\right)^2}\right) + 2\left(\tan^{-1}\eta_r - \tan^{-1}\eta_0\right)\right] & (unstable) \end{cases} \tag{3}$$

Where $\eta_0 = (1-15\zeta_0)^{1/4}$ and $\eta_r = (1-15\zeta_r)^{1/4}, \zeta_0 = z_0/L$

The quasi-laminar resistance is calculated by the following expression

$$R_b = \frac{5Sc^{2/3}}{u_*} \tag{4}$$

Sc is the Schmidt No; equal to the ratio of kinematic viscosity of air and the binary diffusivity of SO_2 and air. The friction velocity (u_*) can be calculated by (Xu and Carmichael, 1998)

$$u_* = \frac{\kappa u(z)}{\ln\left[(z-d)/z_0\right]} \tag{5}$$

The Monin-Obhukov length (*L*), by definition, is the height at which turbulence produced by mechanical and buoyancy forces match. It characterizes atmospheric stability in the surface layer and is positive for a stable atmosphere and negative for an unstable atmosphere. It is determined from the Pasquill Stability classes by the method of Golder (1972) as detailed in Seinfeld and Pandis (2006). The roughness length (z_0) is taken as 1 m as recommended for urban locations by Voldner et al. (1985). The displacement length (d) is 70 – 80% of the height of the large roughness elements (Xu and Carmichael, 1998). The reference height (z) is taken as 10 m and the Von Karman constant (κ) as 0.4.

2.2.2 Surface resistance

The surface or canopy resistance is the most difficult to parameterize due to the complex nature of the processes involved in the absorption and retention of gases by vegetative surfaces. At the same time it is often the dominating resistance especially in the tropics where the atmosphere is highly convective. In recent studies conducted for this region, the parameterization of Wesely (1989) was used to calculate the surface resistance (Seth et al., 2010, Patra and Ghosh, 2010 and Picardo and Ghosh, 2011). It has been used in other studies for Asia as well (Xu and Carmichael, 1998 and Kumar et al., 2008). However, the several advancements made in the science of dry deposition and in the understanding of the dependence of surface resistance on environmental factors have rendered the parameterization of Wesely (1989) somewhat outdated. Many of these advancements are embodied in the work of Zhang et al. (2003b). These include a sunlit/shaded big leaf model for the calculation of the bulk canopy stomatal resistance from the individual leaf resistance via the Leaf Area Index (LAI). LAI is the ratio of leaf surface to ground surface and is around 1 for urban canopies and close to 6 for forests. Sunlit and shaded leaves are treated differently in this canopy -stomatal -resistance model. In Wesely's parameterization (1989), a base bulk stomatal resistance is provided and then modulated with radiation and temperature. This base bulk stomatal resistance value was specified for discrete seasonal categories and over various land types. The problem with this approach is that the seasonal categories considered by Wesely and the corresponding change in the canopy structure do not match the climate and vegetation characteristics in tropical Asia. Specifically, during the winter season at NLC, the temperature is around 25 ^oC and the vegetation is healthy. In contrast the winter seasonal category in Wesely (1989) describes conditions of subzero temperatures and snow covered ground! Moreover, the same land use type (e.g.

agricultural) can also have widely different vegetative characteristics depending on the geographical location. These short comings were realized by Gao and Wesely (1995) who introduced LAI into the stomatal resistance model of Wesely (1989). In Zhang et al. (2003b) all the resistances which are dependent on the canopy structure are related to LAI. This allows an accurate representation of the local vegetative characteristics and the seasonal dependence of green cover. The other improvements in Zhang et al. (2003b) include revised methods of accounting for wet surfaces and their effect on stomatal and non-stomatal resistances and a new parameterization of non-stomatal resistance which considers the effect of meteorological variations (Zhang et. al., 2003a).
For the above mentioned reasons, it was deemed necessary to adopt the parameterization of Zhang et al (2003b) for an accurate and region specific study of dry deposition. The surface resistance is represented as a combination of stomatal and non-stomatal resistances in parallel since stomatal uptake as well as cuticular absorption and deposition onto twigs and the ground occur simultaneously.

$$\frac{1}{R_c} = \frac{1 - W_{st}}{R_{st} + R_m} + \frac{1}{R_{ns}} \tag{6}$$

R_{st} is the canopy stomatal resistance. Stomatal uptake of gaseous species is controlled by the degree of stomatal opening. The major environmental factors which modulate stomatal opening are solar radiation, ambient air temperature, water vapor pressure deficit and leaf water stress. These are accounted for in the canopy resistance model. R_m is the mesophyll resistance which is treated as gas species dependent and specified as 0 for SO_2 since it is highly soluble in water (Zhang et al., 2002). Together they signify the total resistance to stomatal uptake. W_{st} accounts for the blocking of stomata during rains by the film of water which develops on the leaves. However, the net result of rain is a decrease in overall surface resistance since it greatly reduces the non-stomatal resistance (R_{ns}) of the surface in the case of a soluble gas like SO_2. The non-stomatal resistance is a combination of the in-canopy aerodynamic resistance (R_{ac}) and resistance to deposition to the ground (R_g), in series, along with canopy cuticular resistance in parallel (R_{cut}).

$$\frac{1}{R_{ns}} = \frac{1}{R_{ac} + R_g} + \frac{1}{R_{cut}} \tag{7}$$

The presence of wet surfaces due to rain or dew considerably decreases the cuticular and ground resistances. The friction velocity is included in the parameterization of in-canopy aerodynamic resistance, which is one of the advancements of this method. Apart from the canopy stomatal resistance, the LAI also has an effect on the in-canopy aerodynamic resistance and the canopy cuticular resistance. Hence, the LAI is quite an important parameter. The formulae for each of these terms and the parameters based on land use category are given in Zhang et al. (2003b) and Zhang et al. (2002). A large number of land use types are considered and the effect of environmental factors on stomatal conductance is accounted for via formulations which vary with the type of vegetation. Thus it is possible to include region specific information in the model and generate results which are far more compatible to the study area using the method of Zhang et al (2003b). In the present study, NLC is represented by an urban canopy land use type with tropical broadleaf vegetation.

2.2.3 Leaf area index for NLC

As described in the previous section, LAI is a key parameter which captures the local vegetative characteristics and its seasonal dependence. In this work, the LAI over NLC was obtained from MODIS satellite data (product MCD15A2). The data is available in 1 km resolution and is free to download. From the LAI data, which agrees with personal sampling of the vegetation, it was observed that the trees are at their lush best during October, the month of the onset of the NE monsoon and are at their leanest in May which is the peak of the dry summer season. NLC receives some showers from the South West (SW) monsoon as well -this brings relief from the summer heat and causes a rise in LAI from August onwards. Although there is a seasonal variation, there are no bare periods without any green cover- this is in sharp contrast to trees in the mid-latitudes. Moreover, it is comforting to note that the month of the least vegetative cover (i.e. May) is the hottest month when the boundary layer is at its most convective, leading to dilution of pollutants. Values of LAI are available with a spacing of 8 days. The averages for December'08, May'09 and October'09 were calculated as 0.91, 0.54 and 1.06 respectively. Images provided by the MODIS product (MCD15A2) of LAI over the peninsular part of the Indian subcontinent are displayed below (Fig. 3).

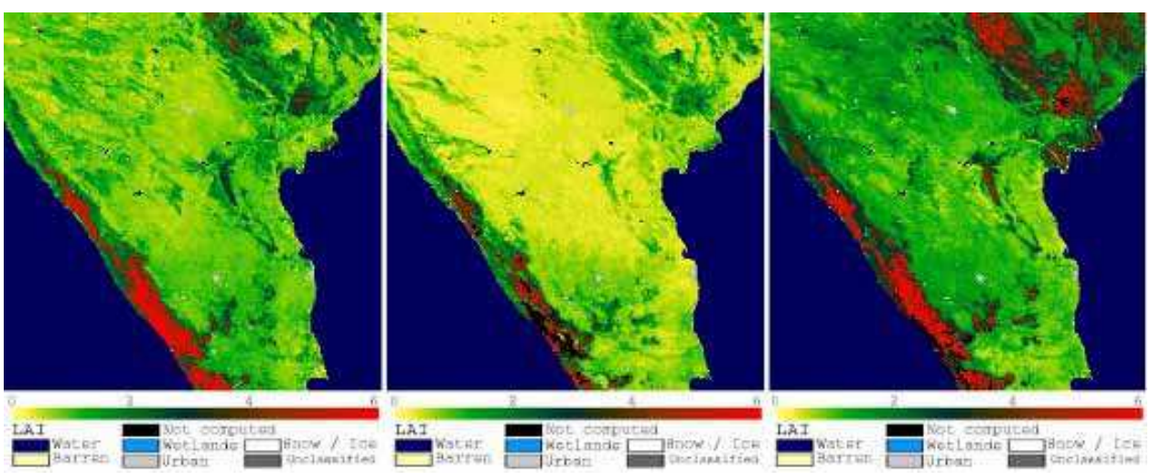

Fig. 3. LAI over the subcontinent for 10th Dec'08, 17th May'09 and 16th October'09 respectively (MODIS MCD15A2)

2.3 Deposition velocity of SO_2 at NLC

2.3.1 Calculation of deposition velocity for three seasons- summer, NE monsoon and mild winter

The average deposition velocity of SO_2 is computed by the method of Zhang et al. (2003b) for the months of December, May and October which represent the three major seasons experienced at NLC- mild winter, hot dry summer and wet North East Monsoon respectively. The statistical mean and standard deviation of the meteorological inputs, namely wind speed, solar radiation and relative humidity as well as the number of rainy days are given in Table 2. It is observed that the temperatures are generally above 25 ^{o}C even during December and that NLC receives considerable solar radiation throughout the year, including the month of October which experiences the maximum rainfall. The computed deposition velocities are presented in Table 3.

The seasonal modulation of the deposition velocity with LAI is apparent. In addition, the rains during October further increase deposition during the day and night due to the presence of wet surfaces on the leaves, twigs and ground. Matsuda et al. (2006) performed field experiments to determine the dry deposition velocity of SO_2 over a tropical forest in Northern Thailand. Although they studied a full fledged forest as opposed to an urban canopy, the vegetative characteristics of the region are similar to our study area. They observed much higher values of SO_2 deposition velocity during the rainy season as compared to the dry season with maximum values of 1.39 cm s^{-1} and 0.31 cm s^{-1} in the wet season and dry season respectively (daytime). They emphasize the importance of accounting for the effect of wet surfaces on non-stomatal resistance in order to accurately model the higher observed values of V_d during the rains. Moreover, they found that the value of deposition velocity predicted for tropical broadleaf trees by Zhang et al., (2003b) during the wet season was consistent with their experimental observations.

Month		**Wind (m s^{-1})**		**Solar radiation (W m^{-2})**		**Temperature (ºC)**		**Relative humidity (%)**		**Rainy Days**
		MEAN	STD	MEAN	STD	MEAN	STD	MEAN	STD	
Dec'08	Day	1.37	0.46	346.12	146.41	28.00	2.00	63.16	2.57	4.00
	Night	0.55	0.39	NA	NA	22.00	0.96	58.77	2.26	
May'09	Day	1.84	1.81	475.45	92.38	36.65	2.36	55.57	5.43	0.00
	Night	1.19	0.65	NA	NA	27.79	1.62	52.91	4.95	
Oct'09	Day	1.64	0.88	416.00	111.69	32.93	1.92	52.57	0.95	13.00
	Night	0.51	0.70	NA	NA	25.20	1.05	50.88	0.35	

Table 2. Meteorological data used for computation of deposition velocity (NA: Not Applicable)

Season	**LAI**	V_d (cm s-1)	
		Day	**Night**
DEC 08- Mild winter	0.91	0.334	0.105
MAY 09- Hot Summer	0.54	0.215	0.145
OCT 09- NE Monsoon	1.06	0.478	0.214

Table 3. Deposition Velocity for the three major seasons at NLC

2.3.2 Variation of deposition velocity with environmental factors

All available parameterizations of deposition velocity are based on experimental observations from numerous field studies. The modulation of the various processes involved in dry deposition by environmental factors is quite complex and while formulations are provided for each individual process, it is difficult to comprehend the overall effect of any individual factor on deposition velocity. In this section, we focus on two

important factors- wind speed and solar radiation and study their effect on deposition velocity as captured by the parameterization of Zhang et al. (2003b).

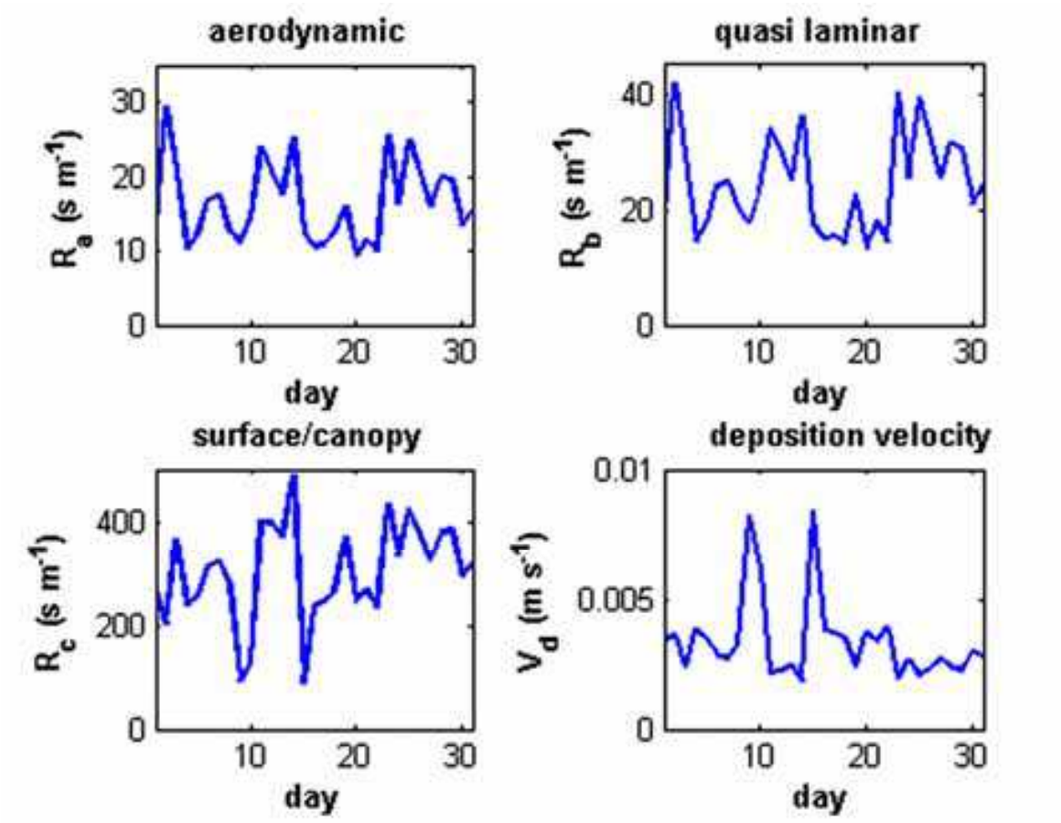

Fig. 4. Resistances and deposition velocity calculated for December 2008 at 14:30 IST

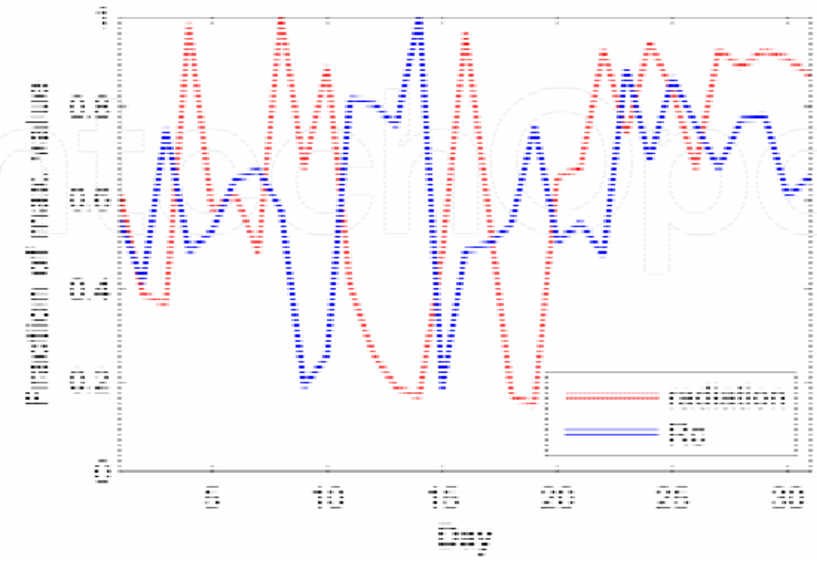

Fig. 5. Variation of canopy resistance with solar insolation (Dec 2008 14:30 IST)

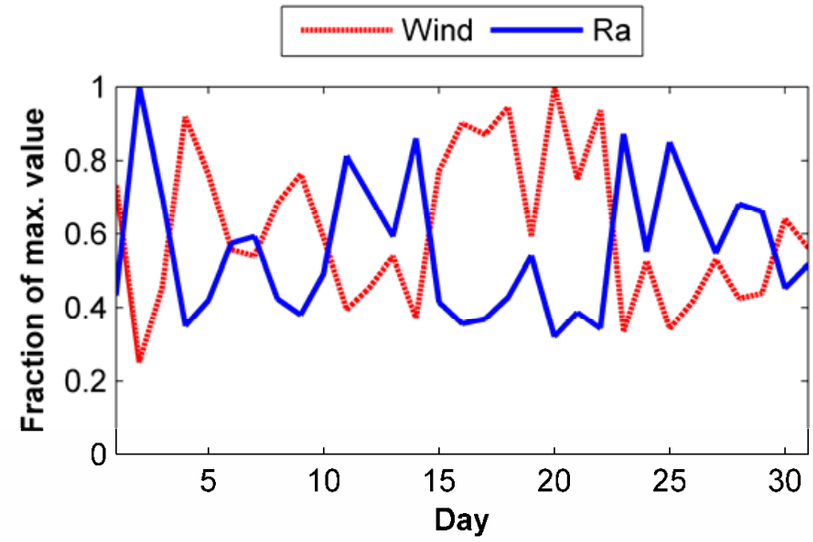

Fig. 6. Variation of aerodynamic resistance with wind speed (Dec 2008 14:30 IST)

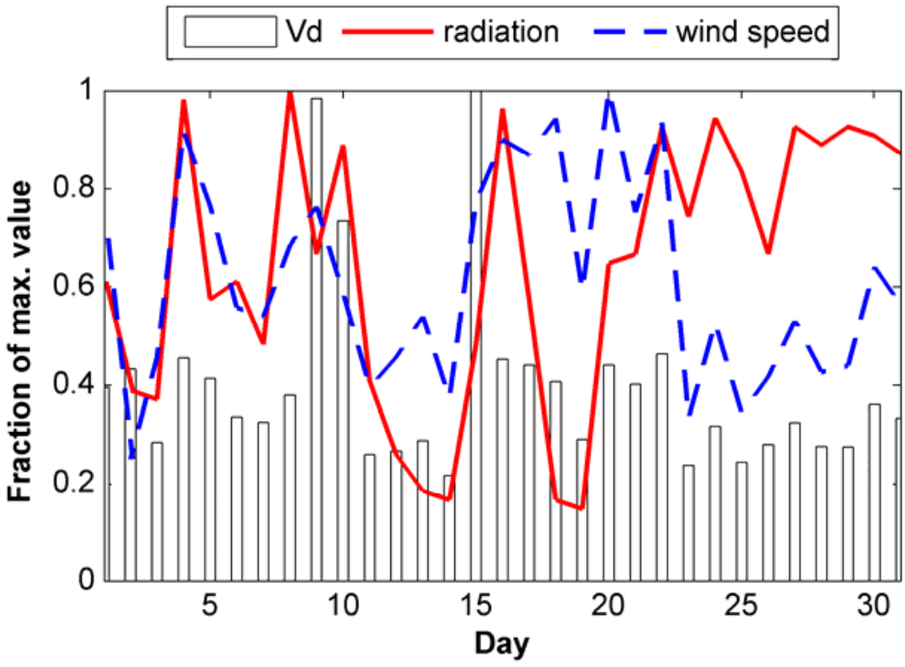

Fig. 7. Variation of deposition velocity with wind speed and solar insolation (Dec 2008 14:30 IST)

The values of the resistances and deposition velocity (V_d) computed for each day of December 2008 at 14:30 (daytime) is shown in Fig. 4. The canopy resistance (R_c) proves to be the controlling resistance in the dry deposition process, accounting for about 80% of the total resistance. Hence one would expect the solar insolation which strongly affects R_c to have a marked affect on V_d as well. This is indeed the case. In fact, the values of V_d are substantially lower at night since there is no solar radiation and the stomata are practically closed (Table 3).

The wind speed modulates R_a and R_b in the same manner. Normalized plots of R_c and R_a with solar radiation and wind speed respectively show an inverse dependence in both cases (Fig 5 and 6). However, while wind speed seems to be the sole important factor in controlling R_a, it is clear that there are significant contributing factors other than solar radiation which affect R_c. Fig. 7 shows the variation of V_d with both environmental factors. The tall standalone peaks correspond to rain and the effect of wet surfaces. A close look at days 12 to 14 seems to suggest that wind speed is the dominant overall factor. This is because, in addition to R_a, the wind also affects R_c by modulating the in-canopy aerodynamic resistance which a species experiences before deposition onto the ground or the lower parts of the trees (please refer Section 2.2.2).

2.4 Cleansing efficacy of the evergreen canopy

The flux of SO_2 to the ground at any location in NLC can be computed from Eq. (1) using the calculated deposition velocity if the concentration at the reference height is known. In the absence of concentration measurements, modelled values can be used to study the removal of SO_2 by the canopy. In this section we investigate the role of the urban canopy in improving air quality, especially in the township. On the 21st of May 2009, a southwest wind transported pollution directly over the township. The wind speed was 2.3 m s^{-1} and the solar radiation was 359 W m^{-2}.This situation provides an ideal setting for our study. However, before analyzing the deposition of SO_2, it is necessary to predict the concentration of SO_2 over the township.

2.4.1 Dispersion model for predicting SO2 concentration

In this study, a tailor made steady state atmospheric gaussian-dispersion model is used which was developed as part of a consultancy with NLC. This model is based on the gaussian plume formula which is applicable to the steady state emission of a gas from an elevated stack with a totally reflecting ground. Although this model does not account for deposition, the error in predicted SO_2 concentrations is relatively small especially since the township is close to the stacks and the source strengths are high. The accuracy is sufficient for the purposes of this study. The gaussian plume equation which predicts the concentration (µg m^{-3}) at any point around the stack is given by:

$$C_g(x,y,z) = \frac{q\times 10^6}{2\pi u\sigma_y\sigma_z}\exp\left(\frac{-y^2}{2\sigma_y{}^2}\right)\times\left[\exp\left(\frac{-(z-h)^2}{2\sigma_z{}^2}\right)-\exp\left(\frac{-(z+h)^2}{2\sigma_z{}^2}\right)\right] \quad (8)$$

The stack is taken to be at the origin with the x axis along the centerline of the plume which is in the mean direction of the wind. The y axis is along the horizontal and the z axis along the vertical. According to this model, as the plume travels with a mean speed u m s^{-1} along the wind direction, it disperses horizontally and vertically so that the average steady state concentration at any cross section of the plume follows the normal Gaussian probability distribution. σ_y and σ_z (in meters) are the standard deviations of the concentration in the y and z directions. q is the source strength (g s^{-1}) and h is the effective stack height (the vertical rise of the plume, before it bends over, added to the physical stack height- m). The dispersion parameters (σ_y and σ_z) depend on atmospheric stability and distance from the stack and are computed using the formulae recommended by Briggs (1973) based on the Pasquill atmospheric stability classes (Turner, 1969) as detailed in Seinfeld and Pandis

(2006). A detailed exposition of gaussian plume dispersion models can be found in Seinfeld and Pandis (2006) and Hanna et al. (1982). This model is also used in the study of wet deposition of pollutants in the latter part of this chapter.

2.4.2 Deposition from a plume

The ground level concentration computed from the dispersion model is shown in Fig. 8. The township is demarcated by a rectangle and the white markers represent the two power stations (TPS1 and TPS2) with TPS1 on the edge of the township. The text markers indicate the locations of air quality monitoring stations. From Fig. 8 it is clear that much of the township experiences concentrations above 10 µg m^{-3}. Areas closer to TPS1 receive higher amounts of the polluting gas and the concentration in the narrow region surrounding the plume centerline exceeds 100 µg m^{-3}.

Due to the presence of the evergreen canopy, there is a continuous deposition of material from the plume onto the trees. This flux is greater in regions of higher concentration and can be evaluated using Eq. (1). Material will be deposited as long as the plume remains aloft over the canopy and the wind direction does not change. Considerable amount of pollution is deposited and contours of the mass flux are shown in Fig. 9. Approximately 1.91 kg of SO_2 is deposited onto the canopy within the township, in an hour. However, this amount is insignificant when compared to the source strength of the emissions from the stacks which continuously pump pollution into the atmosphere (see Table 1). Since the township is very close to TPS 1 there is no perceivable change in the ambient air concentration while the plume remains aloft. However, areas surrounding NLC would benefit as the plume would have travelled a greater distance and much more SO_2 would have been deposited over the canopy which extends beyond the township. This study can be generalized for a wind driven plume, over any part of NLC with a canopy cover.

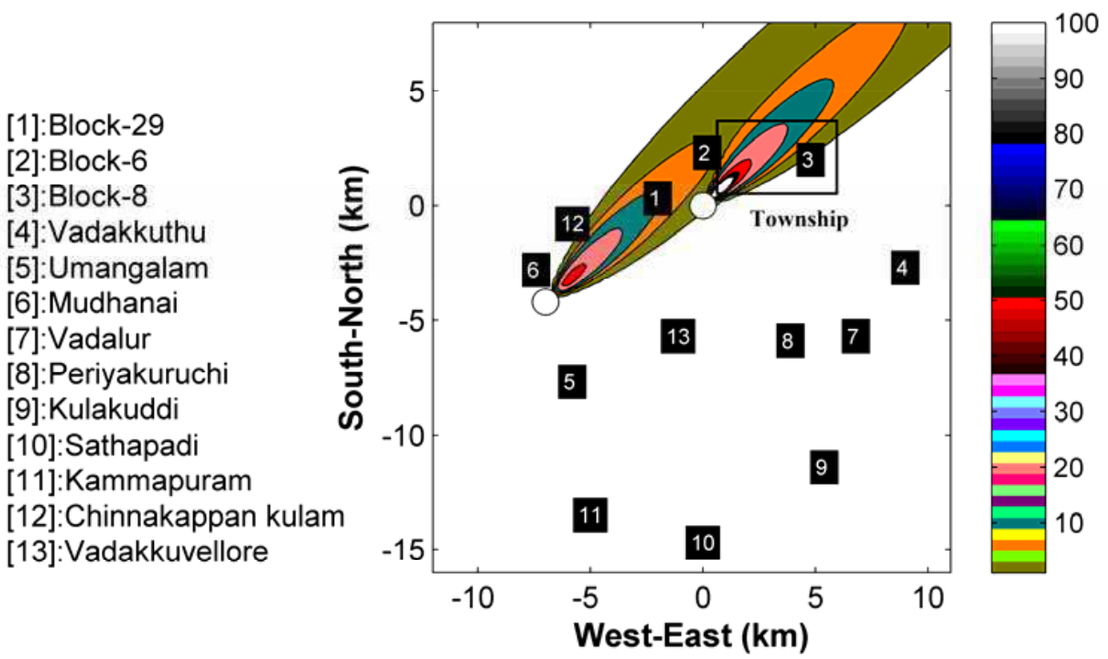

Fig. 8. The modelled ground level concentration over the township on 21st May 2009, 14:30 IST (µg m^{-3})

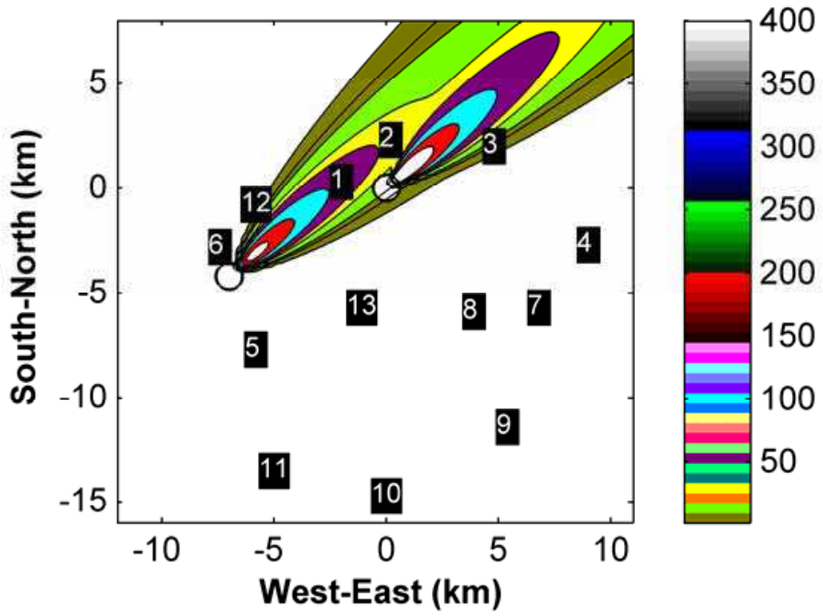

Fig. 9. Mass of SO_2 deposited per unit area per unit time on 21st May 2009, 14:30 IST ($\mu g\ m^{-2}\ hr^{-1}$)

2.4.3 Removal of residual pollution and improvement of air quality

In the previous section the deposition of SO_2 from a plume was analyzed. However, at any time only a small region of NLC can be directly affected by the plume. The other regions will experience residual pollution, left over from a previous visit of the plume or transported from other affected parts of NLC. The trees can reduce the residual SO_2 levels in these regions which do not receive a constant supply of SO_2 for a considerable period of time. These conditions are analogous to those prevalent in cities at night. There is a buildup of pollutants during the day when sources of gaseous pollutants are numerous. At night the emissions subside due to low levels of traffic and urban activity. Since there is no replenishment of pollution, dry deposition onto urban trees can result in improved air quality by the morning. In NLC, this situation is realized when a change in wind direction causes the plume to move away from the township or if a period of calm follows the plume's visit over the township. In either case, SO_2 will be left over the township and diluted by the convective motion of the atmosphere. The mixed layer of the atmosphere, within which this dilution is restricted, is the well mixed region of the atmosphere adjacent to the earth's surface. The height of the mixed layer varies with the time of day, the location of the site (latitude) and the atmospheric stability. The residual SO_2 confined within the mixed layer over the township will be gradually depleted due to dry deposition onto the trees. A first order removal of species from the bottom of a closed stirred tank is a simple way to model this process. A mass balance on SO_2 for a mixed layer of height H_{mix} yields:

$$\frac{dC_g}{dt} = -\frac{V_d C_g}{H_{mix}} \tag{9}$$

This equation when integrated yields the following expression for the time dependent concentration in the mixed layer of the atmosphere, where C_{g0} is the initial residual concentration.

$$C_g(t) = C_{g0} \exp\left(-\frac{V_d t}{H_{mix}}\right) \tag{10}$$

The initial residual pollutant concentration (C_{g0}) can be obtained by first estimating the total amount of pollution left over a given area and then distributing it uniformly throughout the mixed layer. This is done by integrating the plume concentration predicted by the dispersion model throughout the atmosphere for all points within a designated zone (in this case, the township) up to the mixing height and then dividing by the total volume of the region of integration. The present calculation requires an estimation of the height of the mixed layer. This height varies in the summer from 500 m in the morning up to 2-3 km in the late afternoon with an average of 1000 m (Seinfeld and Pandis, 2006). At night the inversion layer is much lower, sometimes only 100 m which can result in high pollution levels. At NLC, this is not much of a concern since the stacks are elevated and most of the pollution is transported above this height. A detailed method for estimating the mixed layer height and its day time variation is given by Luhar (1998). For the purpose of this work, representative values of 1000 m and 500 m are used. The cleansing of the atmosphere over the township due to the removal of SO_2 by the canopy is depicted in Fig. 10. At lower mixing heights, the concentration is much higher, but so is the intensity of the cleansing action. The deposition velocity is low in May and so is the removal of SO_2. However, it is nature's boon that the lowest values of deposition velocity coincide with the hottest month (May) when the day time mixing height is high and pollution episodes are unlikely. This is in contrast to mid-latitudes where the lowest deposition velocity values occur during winter when the mixing height is low. The above calculation is repeated using the deposition velocity of October (Table 3) and the results are depicted in Fig 11. A comparison with Fig. 10 clearly demonstrates the accelerated pace of atmospheric cleansing due to the higher deposition velocity of October.

As mentioned previously, the height of the mixed layer can be very low at night. This can be a problem in polluted cities of developing countries where the majority of emissions have ground sources such as moving vehicles and burning garbage. In such cases the pollutants can become highly concentrated and have a harmful impact on the health of the local population. The presence of pollutant tolerant vegetation can be a mitigating factor as the removal by deposition increases with increase in concentration of the deposition species. The ability of the vegetation to survive under daily pollutant stress is a matter which begs further investigation, especially in context of the continued urbanization in India and other developing countries of Asia. The response of the vegetation may be quite different from that of European and North American plants and calls for another region specific study. The trees at NLC have been able to survive the continuous exposure to the emissions of the power plants but this is, in part, due to the convective atmosphere and the elevated emission sources.

The visionary founders of NLC started an afforestation program several decades ago and now the thriving township is receiving the full benefits of this action. The presence of the green canopy provides a round-the-year removal mechanism for pollutants and thus

contributes to better living conditions in terms of real air quality improvement apart from aesthetic benefits. Pollutants are also removed from the atmosphere by rain. This mechanism is much stronger than dry deposition but is operational for a much shorter time. Wet deposition is dealt with in the next section.

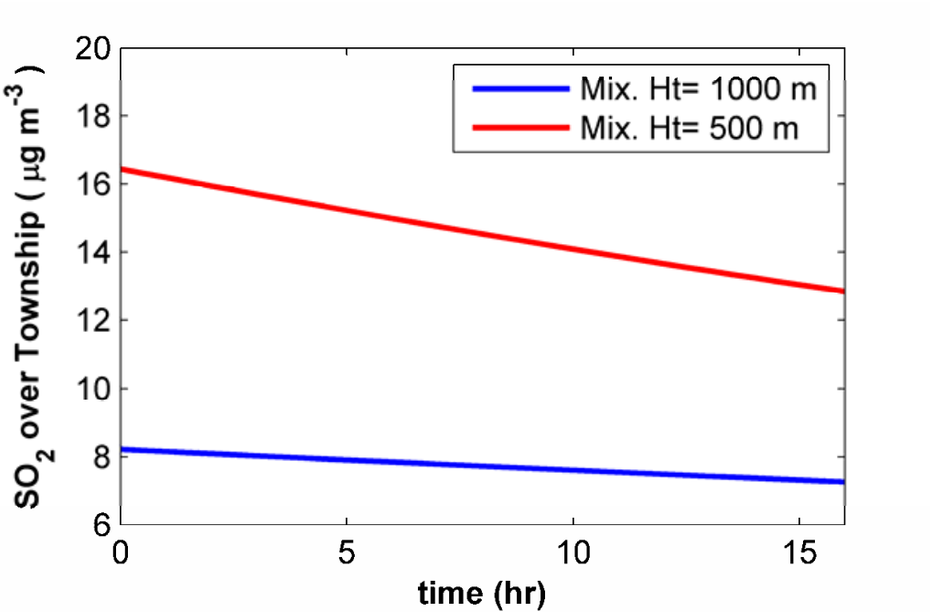

Fig. 10. Depletion of residual SO_2 concentration over the township on 21st May 2009

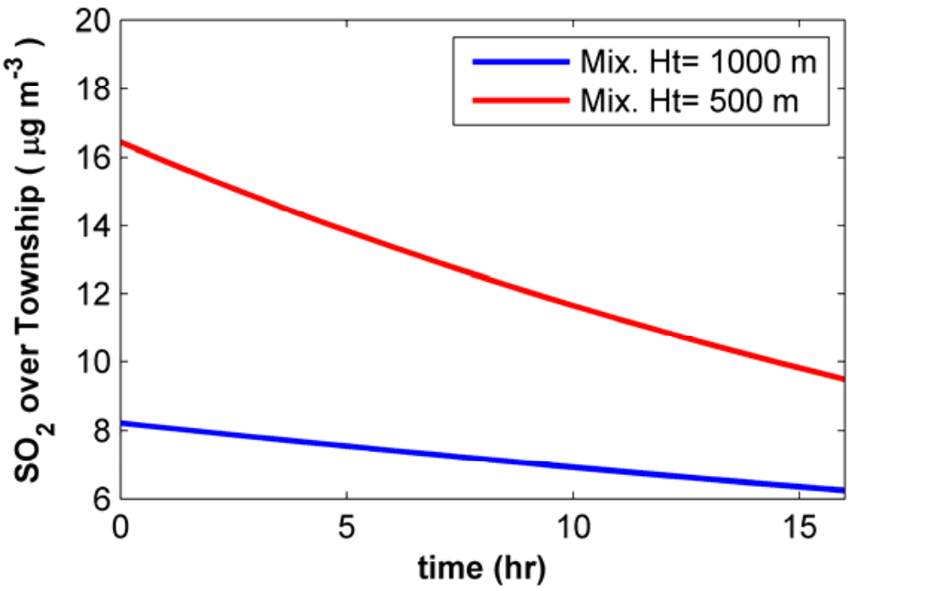

Fig. 11. Depletion of residual SO_2 concentration over the township considering the higher deposition velocity of October

3. Wet deposition- below cloud rain washout

Wet deposition is a broad term encompassing all the natural processes by which material is scavenged from the atmosphere by hydro-elements (cloud and fog drops, snow and rain) and brought to the Earth's surface. Wet deposition mediated by rain, can occur via in-cloud and below cloud scavenging. The former involves in-cloud processes occurring at the cloud base which incorporates substances into the cloud and ultimately transports them to the Earth's surface via rain. The latter, termed Washout refers to the removal of substances from the atmosphere directly by rain drops as they fall from the cloud base towards the ground. We are only concerned with the latter more significant effect.

SO_2 is a water soluble species. During precipitation events, soluble substances in the atmosphere are absorbed by the multitude of falling rain drops and brought to the ground. This process cleanses the atmosphere and leads to an 'after-rain freshness', often experienced by residents of urban and industrialized areas. In order to quantify this phenomenon it is necessary to analyze the mass transfer of a gaseous species into falling rain drops. It must be borne in mind that the drop size is distributed over a range of diameters. Moreover, the drop size distribution (DSD) varies with the geographical location (which inherently includes dependency on the cloud type, cloud base height, local environment etc.) and the intensity of the showers (rain rate). Finally, the results should be linked to the previously described dispersion model (Section 2.4.1) in order to predict the extent of atmospheric cleansing. Washout transports the polluting substance from the atmosphere to the ground. The pollutant is not rendered harmless by transformation or incorporation into a biological cycle (as is the case in dry deposition onto a canopy). This raises the question of pollution at the receptor surface in the form of acid rain. Acid rain is a recognized problem, especially around industrial areas which can cause damage to man-made structures as well as vegetation. Thus, it is important to estimate the pH of the rain water received over NLC.

3.1 Quantification of the rain washout flux

The flux of a gaseous species from the air into rain drops, per unit height of the atmosphere (W, g $m^{-3}s^{-1}$), due to washout by rain, can be approximated by a linear first order relationship (Seinfeld and Pandis, 2006).

$$W = \beta \times C_g \tag{11}$$

β is the scavenging coefficient with units of s^{-1} and C_g is the gas concentration. The flux due to washout (F_W) of a gaseous species to the ground from a column of the atmosphere, of unit cross-sectional area (where the concentration of the gas is horizontally constant), is given by:

$$F_W = \int_0^H (\beta \times C_g)\, dh \tag{12}$$

If the integrated concentration of the species, within a column of the atmosphere, from the ground to the upper reaches of the emissions (H, m) is represented as C_T (g m^{-2}) then for a given value of β(assumed constant at all spatial positions) the flux at any point (x,y) on the ground is given by:

$$F_W(x,y) = \beta \times C_T(x,y) \tag{13}$$

Given the spatially distributed concentration ($C_g(x,y,z)$) around an emission source, which can be obtained using the dispersion model (Section 2.4.1), the concentration at a point is integrated with height to evaluate C_T. With a suitable value of β the flux of species to the ground at that point due to washout by rain is computed.

The above formulation is a first order removal process which considers the rain drops to be a perfect sink, just as the trees were in the dry deposition analysis. However, this assumption is questionable since it is known that SO_2 is not irreversibly soluble and hence the water drop would eventually reach a saturation state after which no further dissolution would be possible. On the other hand, the drops do not fall indefinitely but rather have a finite distance to travel before reaching the ground. Therefore, if during its fall a rain drop remains sufficiently far from saturation, allowing it to absorb SO_2 continuously, then one may consider, for the purposes of this study, that SO_2 is indeed being irreversibly absorbed. A further investigation of this assumption and its validity is presented in the next section which leads on to additional interesting information regarding the relationship between rain drop size and rain water pH.

3.2 Interface mass transfer of SO_2 into a falling rain drop

3.2.1 Transient concentration of dissolved SO_2 inside a falling drop

For effective pollutant washout to occur, a rain drop should absorb pollution through most of its descent. As described in the previous section, it is vital to the description of washout via the scavenging coefficient. For a reversibly soluble gas like SO_2 it is therefore important to calculate the distance through which a drop would fall before saturation.

A rain drop experiences considerable shear at its surface as it falls through the atmosphere which induces internal circulations within the drop. This allows the assumption of a well mixed drop i.e. the concentration gradients within the drop are neglected. The resistance to mass transfer is assumed to exist only in the gaseous film surrounding the drop. It should be noted that if the well mixed assumption was dropped and the liquid phase resistance considered in addition to the gas phase resistance, then this would lead to slower mass transfer with a longer saturation time (Pruppacher and Klett, 1997). Once at the drop surface, the SO_2 dissolves into the drop and is transformed into HSO_3^- ions (bisulphite). Further reaction of these ions to sulphite and other ions is not considered since the dissociation constant is much smaller for any reaction following the initial dissociation to HSO_3^-. With the above assumptions in mind, the process is simplified to the transport of SO_2 in the atmosphere, through a gaseous film surrounding the drop, to the drop surface where SO_2 is absorbed and increases the concentration of HSO_3^- uniformly within the drop (well mixed assumption). This situation is described by the following differential equation (Pruppacher and Klett, 1997).

$$\frac{dC_L}{dt} = \left(\frac{12 f_g D_g^*}{D^2}\right)\left(C_g - \frac{C_L^{\,2}}{K_H K_1 RT}\right) \tag{14}$$

C_L is the HSO_3^- concentration within the drop (mol L^{-1}) and C_g is the SO_2 concentration in the atmosphere. In this equation the units of C_g are mol L^{-1}. However for convenience the ambient air concentration values are reported in μg m^{-3} as was done in section 2 of this

chapter. D is the drop diameter (m), K_H is Henry's Law constant and K_1 is the dissociation constant of the reaction of formation of HSO_3^-. f_g is the ventilation coefficient which is the ratio of the mass transfer of the gas for a drop falling at its terminal velocity to that of a stationary drop. D_g^* is the modified diffusivity ($m^2\ s^{-1}$) which is obtained from the binary diffusivity of SO_2 (D_g, $m^2\ s^{-1}$) in air by the following expression:

$$D_g^* = D_g \Big/ \left[1 + \left(8D_g / D\alpha V_G\right)\right] \tag{15}$$

α, the mass accommodation coefficient, is assumed to be 0.5 for this study (Pruppacher and Klett, 1997) and V_G, the molecular thermal velocity can be computed by (Seinfeld and Pandis, 2006)

$$V_G = \left[8RT/\pi M\right]^{1/2} \tag{16}$$

R is the universal gas constant (8.314 $J\ K^{-1}mol^{-1}$), T is the temperature (K) and M is the molecular mass of the species ($kg\ mol^{-1}$). In this study we are concerned with wet scavenging over the NLC region (approx. 20 km^2) surrounding the source of emissions. Since these emissions are unlikely to reach the cloud base over this region, we can assume the concentration of HSO_3^- in the rain droplets, as they fall from the cloud base, to be negligible. Then the initial condition for Eq. (14) is $C_L = 0$. This first order differential equation can be solved to yield an expression for the transient concentration of HSO_3^- in the drop.

$$C_L(t) = C_{Lsat} \tanh\left(\frac{kC_g t}{C_{Lsat}}\right) \tag{17}$$

C_{Lsat} is the concentration in a saturated droplet which is in equilibrium with the ambient air concentration of SO_2 and

$$C_{Lsat} = \left(C_g K_H K_1 RT\right)^{1/2} \tag{18}$$

k is the average mass transfer coefficient (s^{-1}) which accounts for both collisional as well as diffusional uptake.

$$k = 12 f_g D_g^* / D^2 \tag{19}$$

The value of the ventilation coefficient can be determined from the following empirical relation (Pruppacher and Klett, 1997) in terms of the Reynolds (Re) and Schmidt Numbers (Sc).

$$f_g = 0.78 + 0.308 Sc^{1/3} \mathrm{Re}^{1/2} \tag{20}$$

These dimensionless numbers are defined as:

$$Sc = D_g / \nu, \mathrm{Re} = DU_t / \nu \tag{21}$$

ν is the kinematic viscosity of air. The following relation is used for calculating the terminal velocity (U_t, $m\ s^{-1}$) of a drop (Johnson, 1982) where Q is an empirical constant with a value of 8630 s^{-1}.

$$U_t = Q(D/2) \tag{22}$$

Concentration profiles of HSO_3^- in a drop falling through a SO_2 laden atmosphere, as given by Eq. (17), are plotted in Fig. 12 for various drop diameters. The time of fall, beginning with the first encounter of the drop with SO_2 pollution, is expressed in terms of the distance of fall after evaluating the terminal velocity for the drop from Eq. (22). The values of the parameters used in the above equations are given in Table 4 and are obtained from Pruppacher and Klett (1997). The atmospheric concentration of SO_2 is taken to be 100 μg m^{-3} which is the ambient concentration expected close to the NLC stacks (See Fig. 8).

D_g , Gas Phase diffusivity	14.1×10^{-6} m^2 s^{-1}
M, Molecular Mass SO_2	64×10^{-3} kg mol^{-1}
ν , Kinematic viscosity of air	14.1×10^{-6} m^2 s^{-1}
K_HRT, Henry's law constant product	30 (dimensionless)
K_1 , Dissociation Constant	1.23×10^{-2} mol L^{-1}

Table 4. Values of the parameters used in Eq. (17)

It is observed that the distance through which a drop falls, before it becomes saturated, increases with the drop's diameter. While the small drops (D < 1 mm) saturate in less than 100 m, the moderate sized ones (D~2 mm) fall for 500 m before attaining saturation. It is observed that the average rain-drop diameter is higher for showers of higher precipitation rates. For the high intensity NE Monsoon showers there is a preponderance of moderate to large sized drops. Moreover, the SO_2 in the atmosphere will be concentrated within the plume. Thus, the distance through which the drop falls, while absorbing SO_2, is the plume width alone and not the entire distance from the cloud base to the ground. Further, in regions of high concentration close to the stacks, the plume width will be small. When the plume width is large (100 to 200 m and beyond) the concentrations will be much lower than 100 μg m^{-3} and so the drops will fall through larger distances than shown in Fig. 12 without attaining saturation. With the above considerations in mind it can be safely assumed that the rain drops do not get saturated as they fall through NLC plumes. Hence the rain will wash out SO_2 from the upper reaches of the emitted plume to the ground level and the process can be treated as a first order removal. NLC is one of the largest power plants in Asia-this reasoning prevails for most power plant emissions over the Indian Subcontinent as well as over other countries which receive intense, monsoon-type rains.

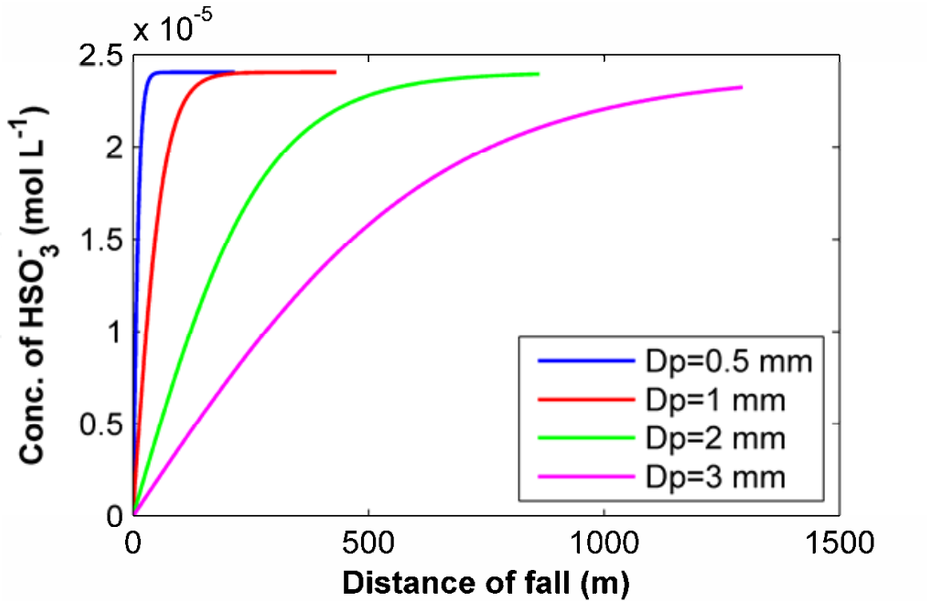

Fig. 12. Concentration of HSO_3^- inside a drop as it falls through SO_2 laden atmosphere with a concentration of 100 µg m^{-3}

3.2.2 Ground level pH of drops over NLC

Apart from the washout of emissions we are also concerned with the acidity of rain water. Thus, it is useful at this stage to compute the pH of the rain drops when they reach the ground. The pH of a rain drop leaving the cloud base (pH_{ini}) is assumed to be 5.6 due to absorption of CO_2 in the upper atmosphere. Applying the principle of electro-neutrality, the increase in H^+ ions due to the absorption of SO_2 and its subsequent dissociation to HSO_3^- ($[H^+]_{abs}$) can be computed. Finally the pH of the drops at the ground can be obtained from the total H^+ ion concentration (pH_{ground}).

$$\left[H^+\right]_{ini} = 10^{(-pH_{ini})}, \qquad \left|pH_{ini} = 5.6\right. \tag{23}$$

$$\left[H^+\right]_{abs} = \left[HSO_3^-\right]_{abs} \tag{24}$$

$$pH_{ground} = -\log_{10}\left(\left[H^+\right]_{ini} + \left[H^+\right]_{abs}\right) \tag{25}$$

The pH of drops of different sizes when they reach the ground is depicted in Fig. 13. The lower flat part of the curve represents drops which get saturated prior to their reaching the ground. They attain a minimum pH of 4.5 which corresponds to the saturation concentration of HSO_3^- in a drop surrounded by a gas phase concentration of 100 µg m^{-3}. The larger sized drops (diameter exceeding 1.5 mm) are unsaturated. The ground level pH of these drops increases with their diameter which suggests that a preponderance of large drops in rain showers will ensure a higher rainwater pH. This result is significant when one realizes that heavier rains have larger drops. However, heavier rains also scavenge more

pollution. The dependence of rain water pH on rain rate will be further analyzed in section 3.4.3.

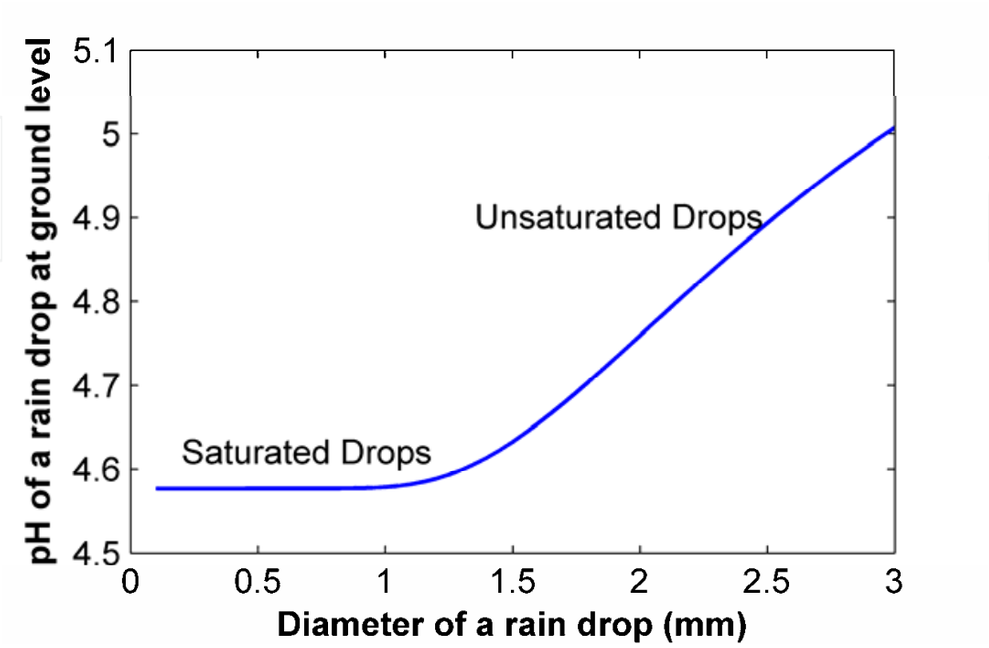

Fig. 13. pH of a drop as it reaches the ground after falling through a SO_2 laden atmosphere with a concentration of 100 µg m^{-3}

3.3 Formulation of the scavenging coefficient for NLC during the NE Monsoons

India receives heavy rainfall from two distinct monsoons. The South West Monsoon bearing moisture from the Indian Ocean, holds sway over most of the Subcontinent from June to September. The North East Monsoon (NE Monsoon) or Retreating Monsoon brings moisture from the Bay of Bengal and empties itself over the South Eastern coast of India during the months of October to December. It is the latter which forms the basis of this study. It is timely as some of the world's mega cities (i.e. Chennai and Kolkata) are along this coastline. The State of Tamil Nadu, located along the South East coastline, is most affected by the NE Monsoon and NLC receives rain rates in excess of 50 mm hr^{-1}.

In order to study washout by the NE monsoons, it is necessary to apply the previous mass transfer study which was aimed at an individual drop, to a multitude of drops of varying size which are present in a rain shower. This is made possible via the formulation of the scavenging coefficient (Section 3.1). For a particular size distributed spectra of rain drops (which varies with rain rate) the scavenging coefficient is given by (Seinfeld and Pandis, 2006):

$$\beta = \int \pi K_C D^2 N(D) d(D) \tag{26}$$

$N(D)$ is the drop size distribution function which represents the number concentration of drops of a given size ($m^{-3}mm^{-1}$). K_c is the empirically determined mass transfer coefficient for the transfer of a gaseous species to falling drops. It can be evaluated by the following

correlation (Bird et. al., 2002). Note that this empirical equation is a form of Eq. (20) and describes the same phenomena of mass transfer to a drop of size D.

$$K_c = \left(D_g/D\right)\left(2 + 0.6Sc^{1/3}\,\mathrm{Re}^{1/2}\right) \tag{27}$$

The DSD (drop size distribution) function ($N(D)$) is determined by fitting experimental data to mathematical distributions. Many different distributions have been used to represent the DSD of rain. These include the Marshal Palmer, Lognormal and the Modified Gamma Distributions. In the work of Konwar *et al*. (2006), it is shown that the Lognormal and Modified Gamma distributions are similar and provide a better fit than the Marshal Palmer distribution for DSD data of rain samples over Gadanki located in Tamil Nadu, India. Moreover, the Modified Gamma distribution is shown to give the best fit for the DSD. Roy *et al*. (2005) have studied the DSD of rain over the Cuddalore district of Tamil Nadu and have fitted the data to the same gamma distribution. Fortunately, NLC, the target area for the application of our work, is located in the district of Cuddalore itself. Assured by the work of Konwar *et al*. (2006) we adopted the gamma distribution of Roy *et al*. (2005) for our study. Curves of the gamma distribution for certain rain rates are shown in Fig. 14. It can be seen that the number of larger drops increases with rain rate. The modified gamma distribution function is given below. N_0, μ and λ are the intercept parameter, shape parameter and slope parameter of this distribution respectively. Roy et al. (2005) fitted DSD data for rain rates ranging from 0.5 mm hr^{-1} to 59 mm hr^{-1}.

$$N\left(D\right) = N_0 D^{\mu} \exp(-\lambda D) \tag{28}$$

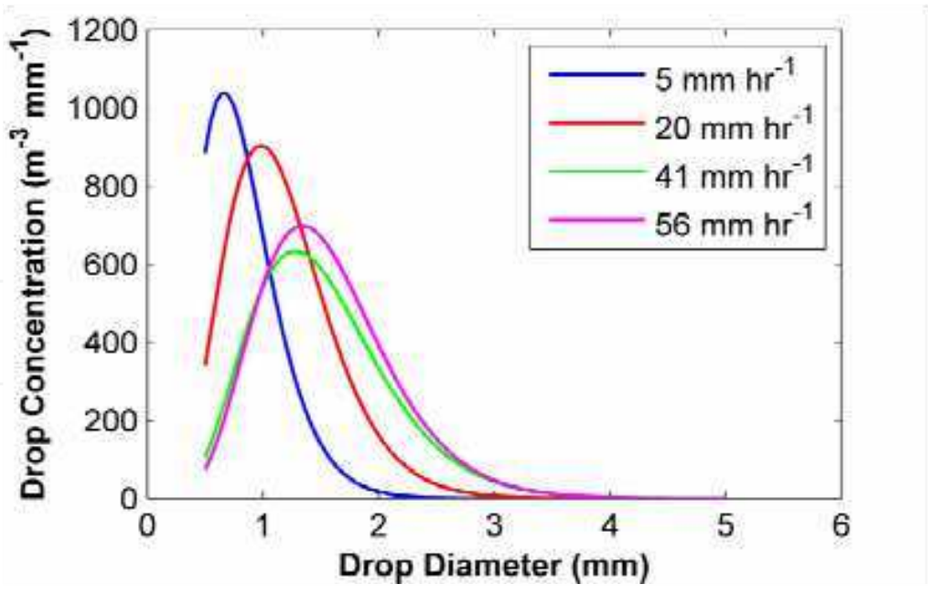

Fig. 14. Modified gamma distribution of rain drop sizes for various rain rates over Cuddalore (Roy et al., 2005)

Knowing the modified gamma distribution function (Eq. (28)), Eq. (26) can be numerically integrated to yield the value of the scavenging coefficient. This is done for all the rain rates

studied by Roy et al. (2005) and the scatter plot shown in Fig. 15 is generated. On specific occasions NLC receives rain rates greater than those studied by Roy et al. (2005), sometimes up to 100mm hr^{-1}. In order to deal with such outlying cases as well as intermediate rain rates, a regression line (Eq. 29) is fitted to the scavenging coefficient results and is used to predict the scavenging coefficient for any rain rate (p, mm hr^{-1}).

$$\beta = \left(2.1961\times10^{-5}\right)p + 1.9244\times10^{-4} \tag{29}$$

Eq. (29) is valid for all non-zero rain rates. It fits the data better within the range of interest as compared to a regression line through the origin (please see Fig. 15).

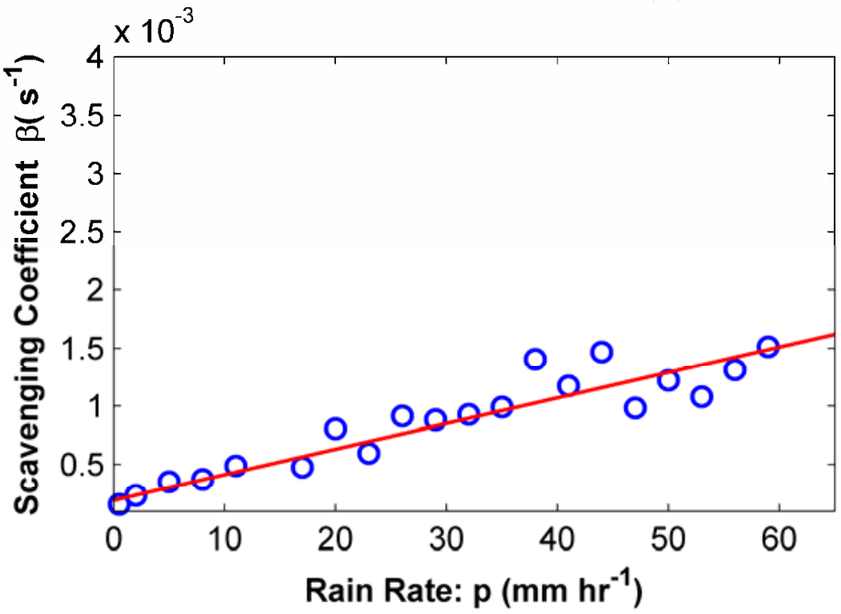

Fig. 15. Scavenging coefficient computed for various rain rates and fitted to a linear regression line

3.4 Atmospheric cleansing due to washout and rain water quality

3.4.1 Incorporation of washout into the dispersion model

In order to determine the reduction in ambient air SO_2 concentration during a rain shower, it is necessary to combine the results of the previous section with the dispersion model that is used to predict the spatially distributed SO_2 concentration around the stacks (section 2.4.1). In fact, the usefulness of applying the scavenging coefficient to analyze washout lies in the ease with which it can be incorporated into a dispersion model to develop a dispersion-deposition model.

During a rain event, a decrease in concentration will occur at all points in the atmosphere and the magnitude of decrease will be proportional to the concentration at that point. This decrease can be accounted for by a reduction in the source strength used in the gaussian dispersion formula (section 2.4.1). This reduction can be approximated by multiplication with an exponential factor which involves the product of the scavenging coefficient and the distance from the stack, along the prevailing wind direction. The washed out concentration is given by (Seinfeld and Pandis, 2006).

$$C_{g,washout}(x,y,z) = \exp\left(-\beta\frac{x}{u}\right)\times\frac{q\times10^{6}}{2\pi u\sigma_y\sigma_z}\exp\left(\frac{-y^2}{2\sigma_y{}^2}\right)\times\left[\exp\left(\frac{-(z-h)^2}{2\sigma_z{}^2}\right)-\exp\left(\frac{-(z+h)^2}{2\sigma_z{}^2}\right)\right] \quad (30)$$

Thus, as a parcel of air travels through rain and away from the stack, the concentration of the soluble gaseous species will be exponentially depleted due to scavenging by the rain. This exponential depletion is a result of the first order removal used to describe washout.
The rain water bearing dissolved SO_2 will reach the ground with an increased acid content. The rain water pH can be evaluated by considering the increase in H^+ ions due to the dissociation of dissolved SO_2 into HSO_3^-, as was done in the case of a single drop (Section 3.2.2). First, the amount of SO_2 brought to the ground per unit area per unit time by the rain is computed using Eq. (13). The volume of rain water received by that surface during a unit of time is simply the rain rate. Thus the concentration of HSO^{3-} ions can be estimated at any location on the ground, which in turn allows a computation of the pH at that point.

3.4.2 Wet deposition of SO_2 over NLC

The model developed in Section 3.4.1 was applied to a typical day in October (specifically 21st Oct 2007) which received heavy showers to the tune of 43.2 mm hr^{-1}. A horizontal wind of magnitude 1.11 m s^{-1} blew in from the north-north-east at the time of the shower. The scavenging coefficient at this rain rate is 1.14×10^{-3} (Eq. (29), Fig. 15). The ground level concentration of SO_2 surrounding the Thermal Power Stations in the absence of rain and the depleted levels due to washout are shown in Fig. 16. It is clear that the sharp NE monsoon showers rapidly cleanse the ambient air. Next, the rain water pH was calculated and contours of the same are displayed in Fig. 17. As may have been expected, the rain water is acidic in the region along the plume centerline (where the atmospheric concentration of SO_2 is maximum) with a pH of 4. However, the ph rises rapidly with distance from the centerline and the three receptors (station 5, 13 and 11 in Fig.17) within the plumes horizontal extent are affected by mild acid rain (pH above 4).

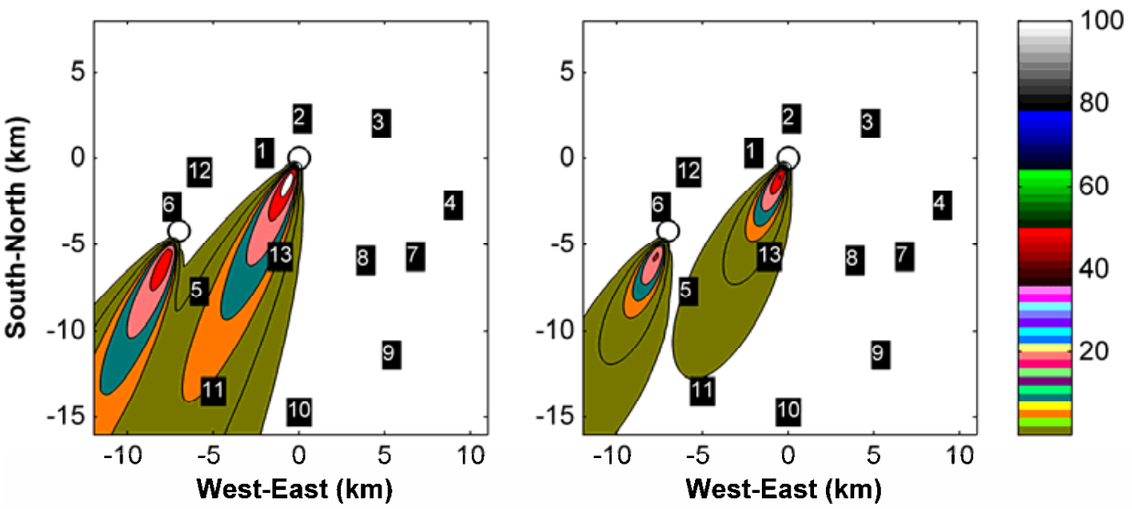

Fig. 16. The SO_2 concentration over NLC before and during the rain showers with rain rate of 43.2 mm hr^{-1}

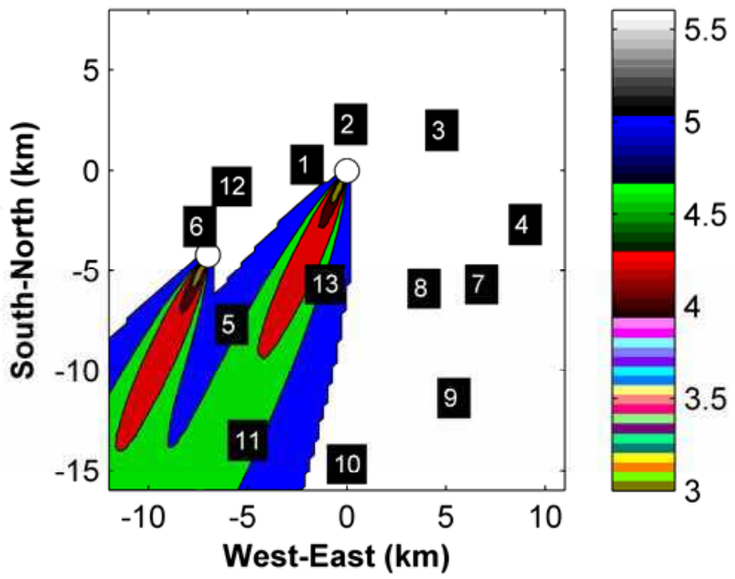

Fig. 17. Contours of the rain water pH at the ground for a rain rate of 43.2 mm hr^{-1}

3.4.3 Dependence of rain water pH on rain rate

It was discussed in section 3.2.2 that the pH of a rain drop increases with its diameter. This suggests that the presence of larger drops in rain showers will result in a higher pH. Further, it was observed in section 3.3 (Fig. 14) that the number concentration of larger drops increases with increase in rain rate. However, it must be borne in mind that higher rain intensities lead to increased scavenging as evidenced by the rising scavenging coefficient with rain rate in Fig. 15. Thus greater amounts of acidic pollutant will be present in the surface rain water. To analyze the relationship between rain rate and rain water pH, the previous computation of pH contours is repeated for an arbitrary small rain rate of 10 mm hr^{-1} and a large rain rate of 100 mm hr^{-1}. The scavenging coefficients at these rain rates are

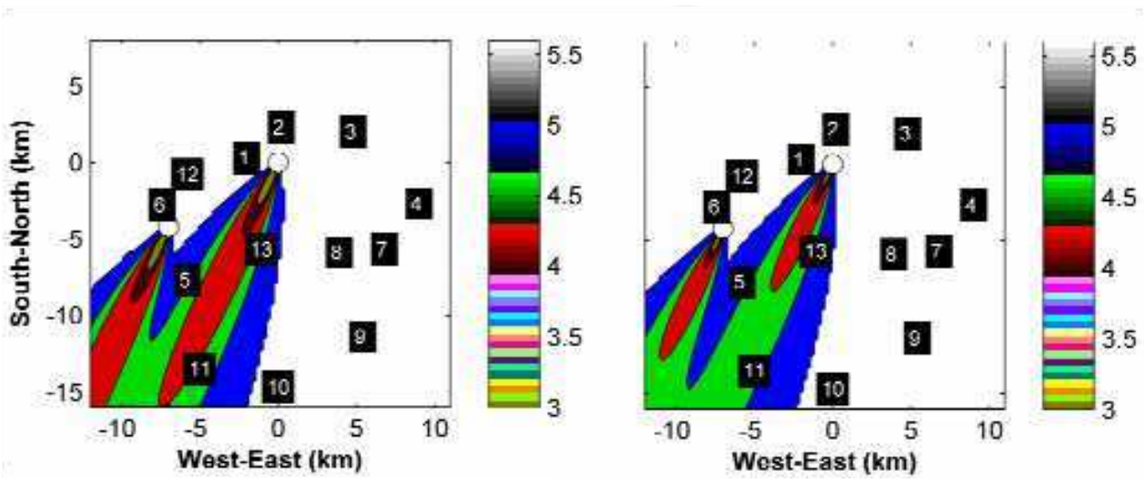

Fig. 18. Contours of the rain water pH for rain rates of 10 mm hr^{-1} (left) and 100 mm hr^{-1}

4.12×10^{-4} s^{-1} and 2.39×10^{-3} s^{-1} respectively (Eq. (29)). The degree of atmospheric cleansing will vary in proportion to the scavenging coefficients and these results are not displayed due to space constraints. The pH contours for rain rates of 10 mm hr^{-1} and 100 mm hr^{-1} are shown in Fig. 18. It is clear from a comparison of these images that the pH of the rain water does increase with rain rate. Although more SO_2 is scavenged at higher rain rates, it is diluted in larger amounts of water. Thus, the heavy rains of the NE monsoon will result in surface rain water of a higher pH as compared to mild mid-latitude precipitation.

4. Conclusion

At the end of the first decade of the twenty first century, the developing nations of the world are in a quandary. Constant industrialization and rising per capita energy consumption implies increasing fossil fuel derived energy usage. In most countries, renewable energy sources alone will not be able to meet the exorbitant energy demands in the foreseeable future. At the same time, the pollution caused by toxic emissions from thermal power plants and industries can no longer be ignored. Sustainable development implies the maintenance of a delicate balance between human progress and conservation/promotion of Nature. Environmental impact assessment studies of new and existing projects form an important component of the roadmap to sustainability. Such studies often turn to mathematical modelling methods for analyzing the impacts of polluting releases, especially gaseous emissions in the context of thermal power plants. Thus far, most studies in Asia have resorted to borrowing results from mid latitude analyses or adopting hasty adaptations of models which were developed for regions quite unlike their own. The widely different climatology, ecology and general environment of the Asian region demands region specific studies and analyses.

In this work a detailed modelling study of the removal mechanisms of gaseous pollutants is presented for the Neyveli Lignite Corporation (NLC), located in Tamil Nadu, India. Removal of SO_2 via dry deposition and rain scavenging is addressed with a particular emphasis on using local meteorological data and determining region specific model parameters. At various points in the analysis, it was observed that nature had provided the region with several advantages as far as mitigation of pollution was concerned. These include the fact that the leanest state of the vegetative canopy coincides with the hot summer when the convective boundary layer will ensure dilution of polluting emissions. The presence of two monsoonal seasons and the heavy rain rates (with larger rain drops) which result in higher pH is another boon to the region. This study is an example of the important inferences that can result from region specific studies that may be missed if unsuitably adapted, borrowed models are used.

While it was demonstrated that the canopy acts as a round-the-year sink for SO_2 and is able to improve air quality and living conditions of the residents, it is yet a matter of speculation as to the effect of continuous exposure to SO_2 on the plants. These plants will have different responses when compared to plants in other continents and should be investigated accordingly. It would be interesting to ascertain whether the monsoon rain received by the Indian sub-continent has larger drop sizes when compared to rain of similar intensity in other parts of the world e.g. Brazil. Most importantly, it is hoped that more such studies are carried out in developing countries where sustainable development is as yet only an ideal and Nature's resilience is constantly put to the test.

5. Acknowledgements

We thank the Neyveli Lignite Corporation (NLC) for funding this work and providing necessary meteorological data. We also thank the Director, School of Mechanical and Building Sciences, VIT University.

6. References

Bird, R. B.; Stewart, W. E. & Lightfoot, E. N. (2002). *Transport Phenomena, 2nd Ed.*, John Wiley (Asia), Singapore, pp. 681

Gao, W. & Wesely, M. L. (1995). Modeling Gaseous Dry Deposition over Regional Scales with Satellite Observations-I. Model Development, *Atmospheric Environment*, Vol. 29, No. 6, pp. 727-737

Hanna, S. R.; Briggs, G. A. & Hosker, Jr. R. P. (1982). *Handbook on Atmospheric Diffusion*, DOE TIC-11223, Technical Information Center, U.S. Dept. of Energy, USA, pp. 25-35

Johnson, D. (1982). The Role of Giant and Ultragiant Aerosol Particles in Warm Rain Initiation. *J. Atmos. Sci.,* Vol. 6, pp. 448-460

Konwar, M.; Sarma, D. K.; Das, J. & Sharma, S. (2006). Shape of the Rain Drop Size Distributions and Classification of Rain Type at Gadanki. *Indian J. Radio Space*, Vol. 35, pp. 360-367

Kumar, R.; Srivastava, S. S. & Kumari, K. M. (2008). Modeling Dry Deposition of S and N Compounds to Vegetation. *Indian J. Radio Space*, Vol. 37, pp. 272-278

Luhar, A. K. (1998). An Analytical Slab Model for the Growth of the Coastal Thermal Internal Boundary Layer under Near-Neutral Onshore Flow Conditions. *Boundary-Layer Meteorology*, Vol. 88, pp. 103-120

Matsuda, K.; Watanabe, I.; Wingpud, V.; Theramongkol, P. & Ohizumi, T. (2006) Deposition Velocity of O_3 and SO_2 in the Dry and Wet season above a Tropical Forest in Northern Thailand. *Atmospheric Environment*, Vol. 40, pp. 7557-7564

NASA, MODIS LAI/FPAR product, Available from: http://modis.gsfc.nasa.gov/

Patra, S. & Ghosh, S. (2010) Quantifying Trace Gas Uptake Rates by Passion Flower Draped Facades and Roofs. *Proc. World Green Roof Congress*, London, 2010

Picardo, J. R. & Ghosh, S. (2011). Establishing the Efficacy of the Cleansing Action of Tropical Evergreens: A Modeling Analysis of Asia's Largest Lignite based Power Plant. *Proc. 1st EnvironmentAsia International Conference*, Bangkok, Thailand, 2011.

Pruppacher, H. R. & Klett J. D. (1997). *Microphysics of Clouds and Precipitation, 2nd Ed.*, Dordrecht, The Netherlands, Kluwer Academic Publishers, pp. 770-772

Roy, S. S.; Datta, R. K.; Bhatia R. C. & Sharma A. K. (2005). Drop Size Distributions of Tropical Rain over South India. *Geofizika*, Vol. 22, pp. 105-130

Seinfeld, J. H. & Pandis, S. N. (2006). *Atmospheric Chemistry and Physics, 2nd ed.* John Wiley, New Jersey, USA, pp. 828-979.

Seth, U. K.; Sarkar, S.; Bardhan, R. & Ghosh, S. (2010). Asia's Largest Lignite based Power Plant's success story: Efficient Removal of SO_2 through a Manmade Forest Canopy. *Proc. World Congress of Engineering*, Imperial College, London, No. 2

Wesely, M. L. (1989). Parameterization of Surface Resistance to Gaseous Dry Deposition in Regional Scale Numerical Models. *Atmospheric Environment*, Vol. 23, pp. 1293-1304

Xu, Y. & Carmichael G. (1998). Modeling the Dry Deposition Velocity of Sulphur Dioxide and Sulphate in Asia. *Journal of Applied Meteorology*, Vol. 37, pp. 1084-99

Zhang, L.; Moran, M. D.; Markar, P. A.; Brook, J. R. & Gong, S. (2002). Modelling Gaseous Dry Deposition in AURAMS: a Unified Regional Air Quality Modelling System. *Atmospheric Environment*, Vol. 36, pp. 537-560

Zhang, L.; Brook, J. R. & Vet, R. (2003a). Evaluation of a Non-Stomatal Resistance Parameterization for SO_2 Dry Deposition. *Atmospheric Environment*, Vol. 37, pp. 2941-2947

Zhang, L.; Brook, J. R. & Vet, R. (2003b). A Revised Parameterization for Gaseous Dry Deposition in Air Quality Models. *Atmos. Chem. Phys.*, Vol. 3, pp. 2067-2082

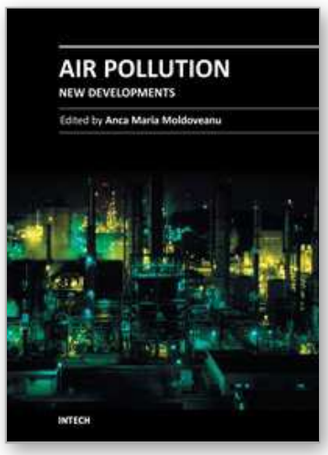

Air Pollution - New Developments

Edited by Prof. Anca Moldoveanu

ISBN 978-953-307-527-3
Hard cover, 324 pages
Publisher InTech
Published online 06, September, 2011
Published in print edition September, 2011

Today, an important issue is environmental pollution, especially air pollution. Due to pollutants present in air, human health as well as animal health and vegetation may suffer. The book can be divided in two parts. The first half presents how the environmental modifications induced by air pollution can have an impact on human health by inducing modifications in different organs and systems and leading to human pathology. This part also presents how environmental modifications induced by air pollution can influence human health during pregnancy. The second half of the book presents the influence of environmental pollution on animal health and vegetation and how this impact can be assessed (the use of the micronucleus tests on TRADESCANTIA to evaluate the genotoxic effects of air pollution, the use of transplanted lichen PSEUDEVERNIA FURFURACEA for biomonitoring the presence of heavy metals, the monitoring of epiphytic lichen biodiversity to detect environmental quality and air pollution, etc). The book is recommended to professionals interested in health and environmental issues.

How to reference

In order to correctly reference this scholarly work, feel free to copy and paste the following:

J. R. Picardo and S. Ghosh (2011). Removal Mechanisms in a Tropical Boundary Layer: Quantification of Air Pollutant Removal Rates Around a Heavily Afforested Power Plant, Air Pollution - New Developments, Prof. Anca Moldoveanu (Ed.), ISBN: 978-953-307-527-3, InTech, Available from: http://www.intechopen.com/books/air-pollution-new-developments/removal-mechanisms-in-a-tropical-boundary-layer-quantification-of-air-pollutant-removal-rates-around

INTECH
open science | open minds

InTech Europe
University Campus STeP Ri
Slavka Krautzeka 83/A
51000 Rijeka, Croatia
Phone: +385 (51) 770 447
Fax: +385 (51) 686 166
www.intechopen.com

InTech China
Unit 405, Office Block, Hotel Equatorial Shanghai
No.65, Yan An Road (West), Shanghai, 200040, China
中国上海市延安西路65号上海国际贵都大饭店办公楼405单元
Phone: +86-21-62489820
Fax: +86-21-62489821

IntechOpen